Supporting Information (SI)

Characterization and purification of the ionic liquid Cyphos IL 101 by non-aqueous solvent extraction

Vincent Cool[†], Sofia Riaño[†], Tom Van Gerven[‡], Koen Binnemans[†]*

[†] KU Leuven, Department of Chemistry, Celestijnenlaan 200F, P.O. box 2404, B-3001 Leuven, Belgium.

[‡] KU Leuven, Department of Chemical Engineering, Celestijnenlaan 200F, P.O. Box 2424, B-3001 Leuven, Belgium.

*Corresponding author:

Email: Koen.Binnemans@kuleuven.be

Table of contents

C101 batches

Table S1. Information of C101 batches.

Reference number in text	Supplier	Batch ID
1	CYTEC	NF17I1208
2	CYTEC	NF23C1799
3	CYTEC	WEE052680
4	CYTEC	WEG030981
5	CYTEC	Unknown
6	IoLiTec GmbH	L0002504-3I0006
7	IoLiTec GmbH	N000249.4.9-IN-0006

LC-MS method

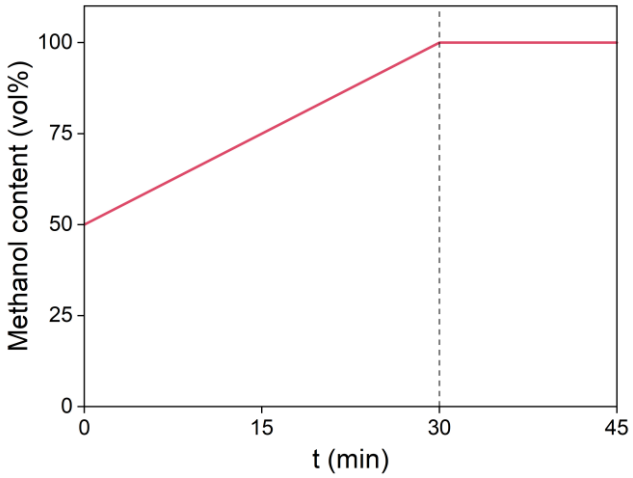

Figure S1. Gradient elution profile used during LC-MS analysis. All mobile phases contained 0.1 mol·L^{-1} formic acid to promote ionization.

Determination of settling velocity

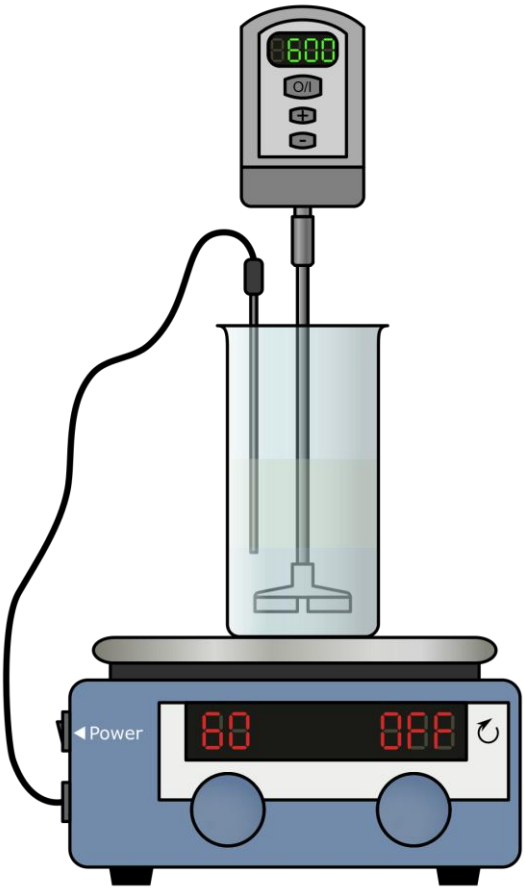

Figure S2. Experimental setup used for determination of settling velocities.

Agitated counter-current column setup

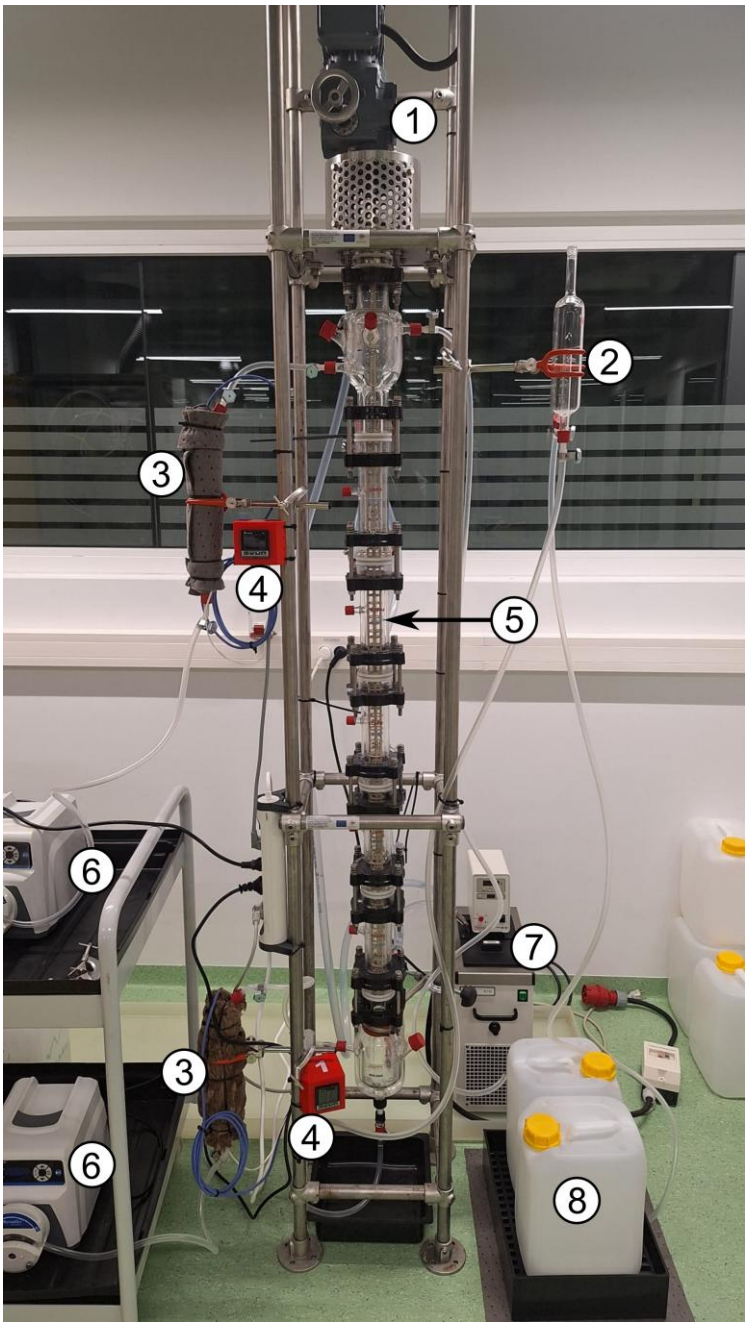

1.	Turbine agitator	**5.**	PEEK rotor-stator assembly
2.	Siphon	**6.**	Peristaltic pump
3.	Heater with isolation	**7.**	Water bath
4.	PID controller	**8.**	Collection vessels

Figure S3. Experimental setup of the Kühni ECR32 laboratory column for C101 purification.

Extracted ion chromatograms part 1

The observation that the signal of *m/z* = 287.3 is nearly equal in intensity to that of *m/z* = = 399.4 is unexpected (Figure S4). Based on the synthetic route of Cyphos IL 101, trihexylphosphonium chloride (*m/z* = 287.3) should be a major impurity, whereas dihexyltetradecylphosphonium chloride (*m/z* = 399.4) is highly unlikely to form. Since these species are homologues, only minor differences in MS response would be anticipated, making the comparable intensities unusual.

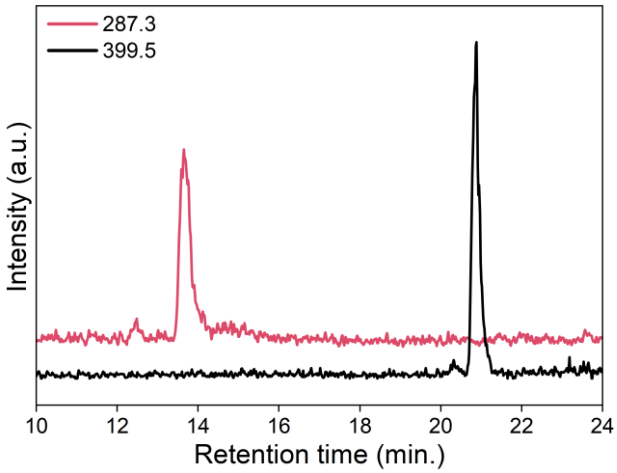

Figure S4. Extracted ion chromatogram of *m/z* = 287.3 and 399.5.

LC-MS analysis using acetonitrile

Using acetonitrile instead of methanol as the diluent and eluent resulted in a dominant signal with *m/z* = 287.3 at 4.68 and 5.36 minutes (Figure S5), with an intensity consistent with its relative abundance. Under these conditions, no co-eluting *m/z* = 317.3 signal was observed. However, two small signals at the same mass appeared slightly earlier at 4.02 and 4.62 min. The origin of this feature remains unclear but suggests the presence of an additional species as a result of its distinct elution time. Closer examination of the methanol-based results also reveals a minor peak in between the dominant signals of hexan-2-yldihexylmethoxyphosphonium chloride and trihexylmethoxyphosphonium chloride (Figure S6). Given its slightly faster elution rate compared to trihexylmethoxyphosphonium chloride in both solvents, the signal can be attributed to the same species.

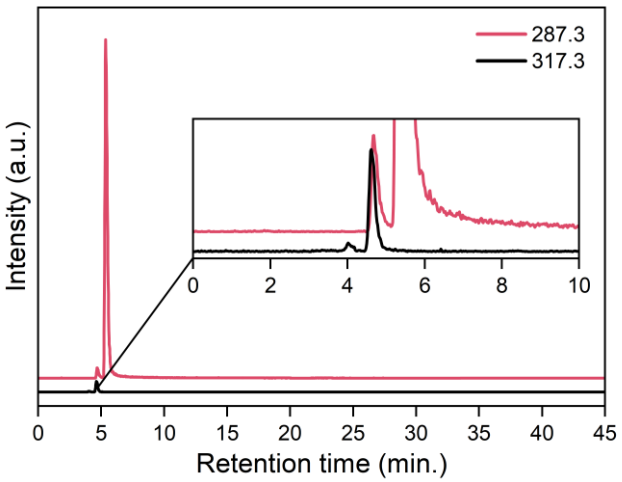

Figure S5. Extracted ion chromatogram of *m/z* = 287.3 and 317.3. Conditions: eluent A = H_2O + 0.1 mol·L^{-1} formic acid; eluent B = acetonitrile + 0.1 mol·L^{-1} formic acid; 1 g·L^{-1} neat C101 dissolved in acetonitrile.

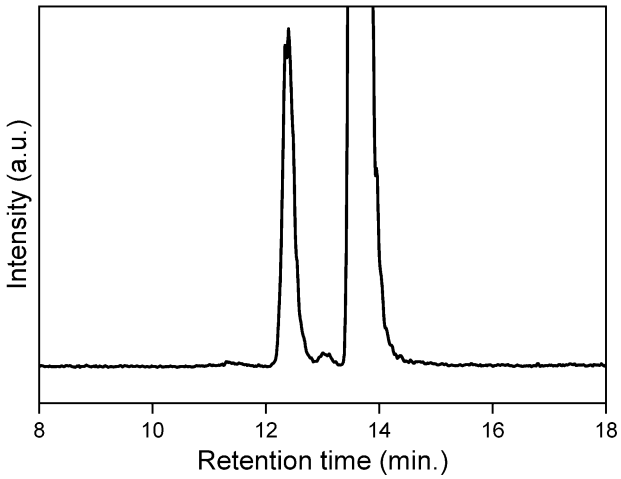

Figure S6. Extracted ion chromatogram of *m/z* = 317.3. Conditions: eluent A = H_2O + 0.1 mol·L^{-1} formic acid; eluent B = methanol + 0.1 mol·L^{-1} formic acid; 1 g·L^{-1} neat C101 dissolved in methanol.

Extracted ion chromatograms part 2

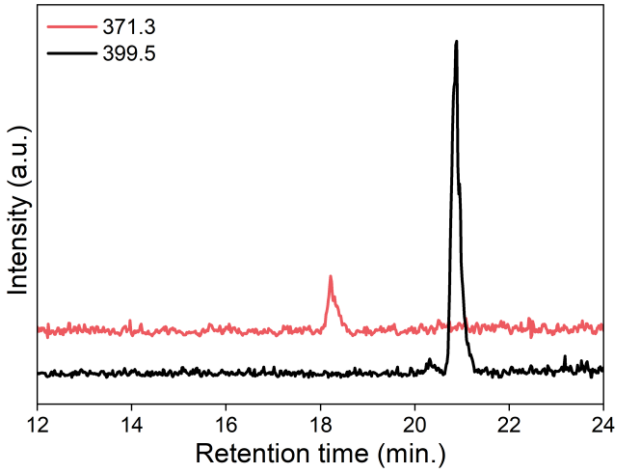

Figure S7. Extracted ion chromatograms of dodecyldihexylphosphonium chloride (*m/z* = 371.3) and dihexyltetradecylphosphonium chloride (*m/z* = 399.5).

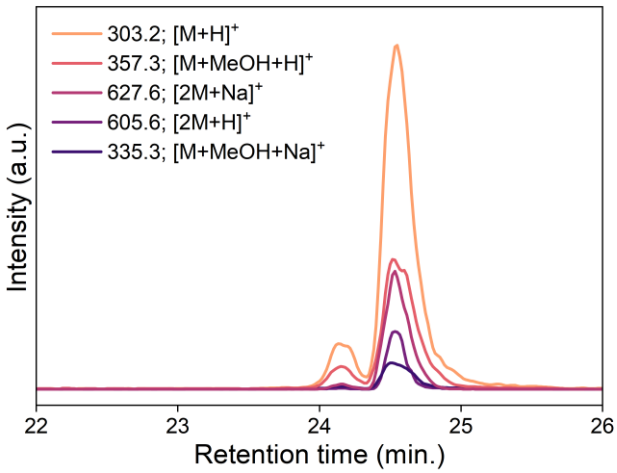

Figure S8. Extracted ion chromatograms of trihexylphosphane oxide and its isomer, hexan-2-yldihexylphosphane oxide. Five distinct masses were detected, each associated with these species.

A distinct dip in the baseline at approximately 26.2 minutes is observed in the chromatogram of *m/z* = 219.2 (Figure S9) and consistently appears across all detected masses. This feature is attributed to detector saturation, resulting from the high concentration of the main trihexyltetradecylphosphonium cation eluting at that time.

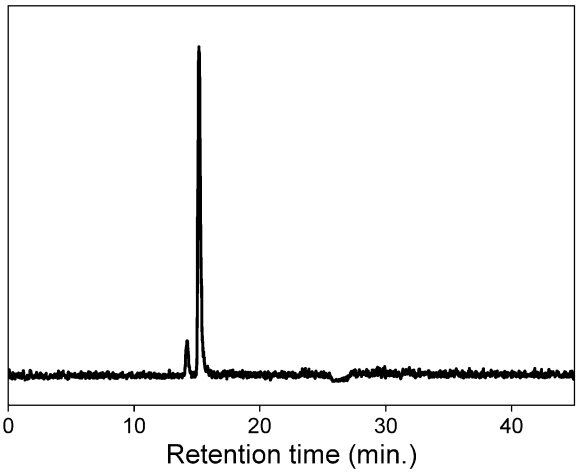

Figure S9. Extracted ion chromatogram of hexan-2-ylhexylphosphane oxide and dihexylphosphane oxide (*m/z* = 219.2).

The chromatogram of *m/z* = 319.3 contains several signals in addition to the one corresponding to hexyldihexylphosphinate (Figure S10). Notably, two major signals are observed at 12.4 and 13.6 minutes. These signals originate from the hexan-2-yldihexyl-methoxyphosphonium chloride and trihexylmethoxyphosphonium chloride compounds (*m/z* = 317.3; Figure S11). As a result of the natural isotopic distribution of ^{13}C and ^{2}H among the 19 carbon and 42 hydrogen atoms in these molecules, additional signals appear at *m/z* = 318.3 and 319.3. The relative abundances of these peaks closely match the theoretical distribution, confirming that these signals arise from the isotopologues rather than distinct chemical species (Figure S12). The abundancy of the signal of *m/z* = 319.3 at 12.4 minutes was found to be slightly overestimated compared to the interval of the distribution based on the IUPAC data. This overestimation can be related with the limited signal to noise ratio obtained for this signal causing an overestimation when the signal is integrated.

Beside the signals at 12.4 and 13.6 minutes, two additional small signals were found at approximately 19.4 and 25.05 minutes. The origin of these signals remains unresolved but the signal of 25.05 minutes might be related with the presence of the hexan-2-yl isomer of hexyldihexylphophinate.

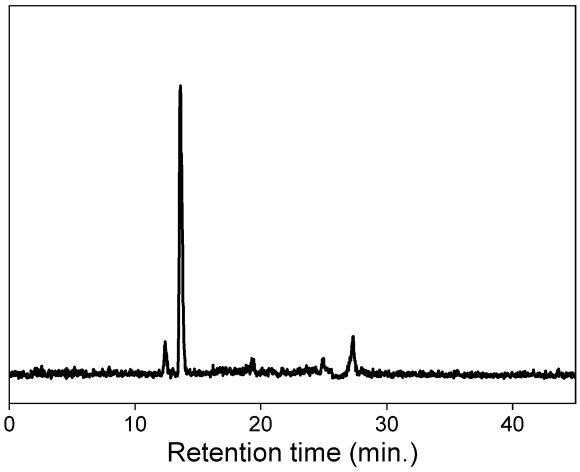

Figure S10. Extracted ion chromatogram of *m/z* = 319.3.

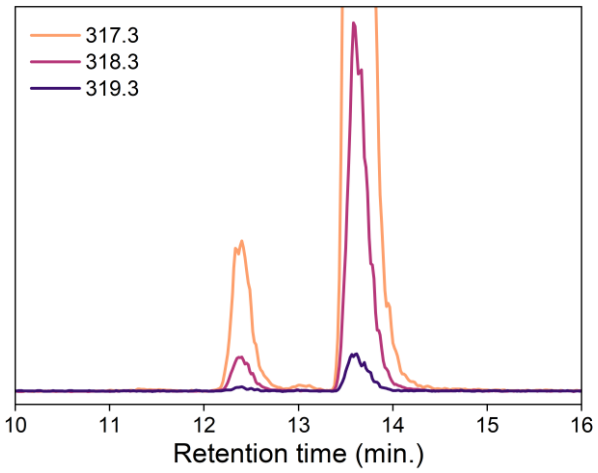

Figure S11. Extracted ion chromatogram of *m/z* = 317.3, 318.3 and 319.3.

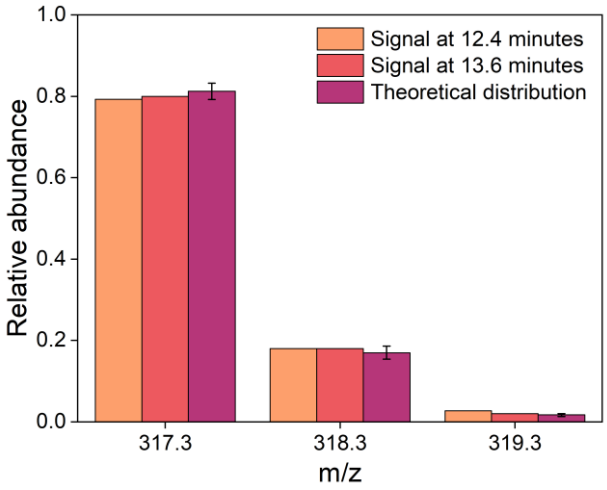

Figure S12. Comparison of the experimental relative abundances with the theoretical distribution of *m/z* =. The theoretical distribution was calculated using isotopic data for hydrogen and carbon from Meija et al.[1] Error bars on the theoretical values represent the range of relative abundances based on natural variation in isotope composition (^{2}H: 0.00001 – 0.00028; ^{13}C: 0.0096 – 0.0116). Any isotopologue beyond *m/z* = 319.3 was not taken into account as their relative abundance represent 0.1% or lower.

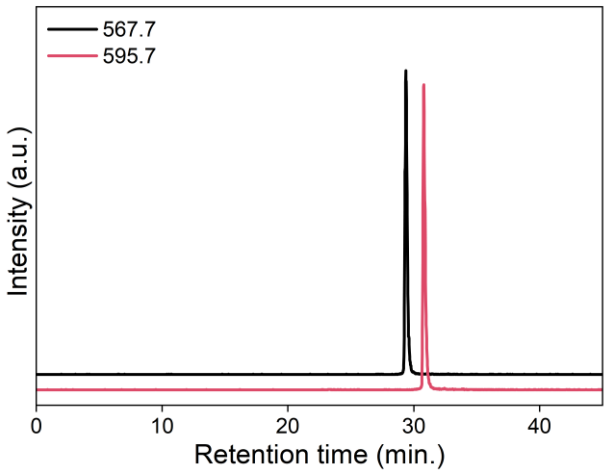

Figure S13. Extracted ion chromatogram of dodecyldihexyltetradecylphosphonium chloride (*m/z* = 567.7) and dihexylditetradecylphosphonium chloride (*m/z* = 595.7).

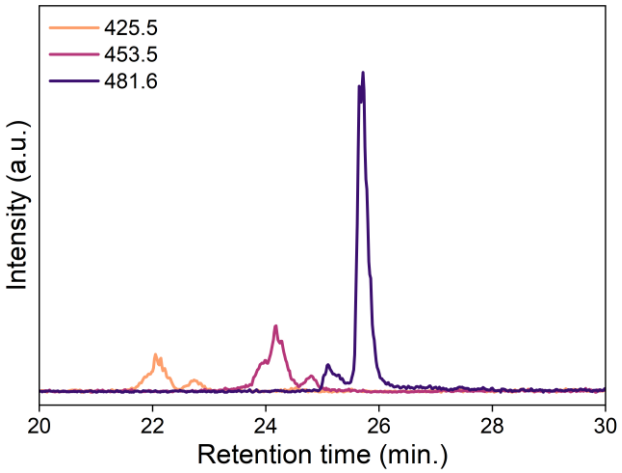

Figure S14. Extracted ion chromatogram of *m/z* = 425.5, 453.5, and 481.6.

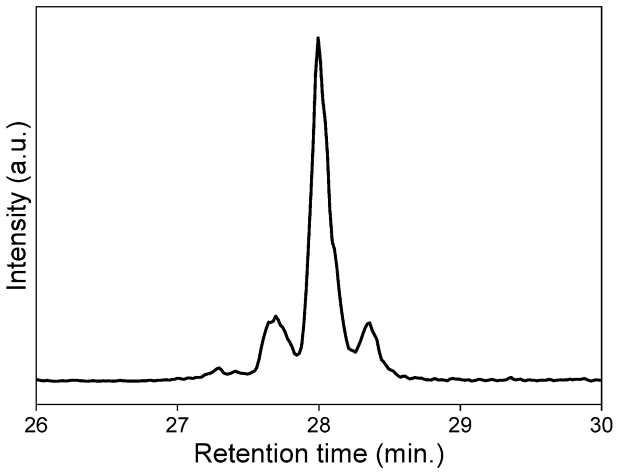

Figure S15. Extracted ion chromatogram of *m/z* = 511.6.

Multiple isomers as a result of multiple hexadiene and hexyne impurities

Several hexadiene and hexyne impurities are commonly present in 1-hexene, including 1,5-hexadiene, 1,4-hexadiene, 1,3-hexadiene, 2,4-hexadiene, 1-hexyne, 2-hexyne, and 3-hexyne.[2,3] As a result, multiple unsaturated phosphonium species can form during the synthesis of Cyphos IL 101 (Figure S16).

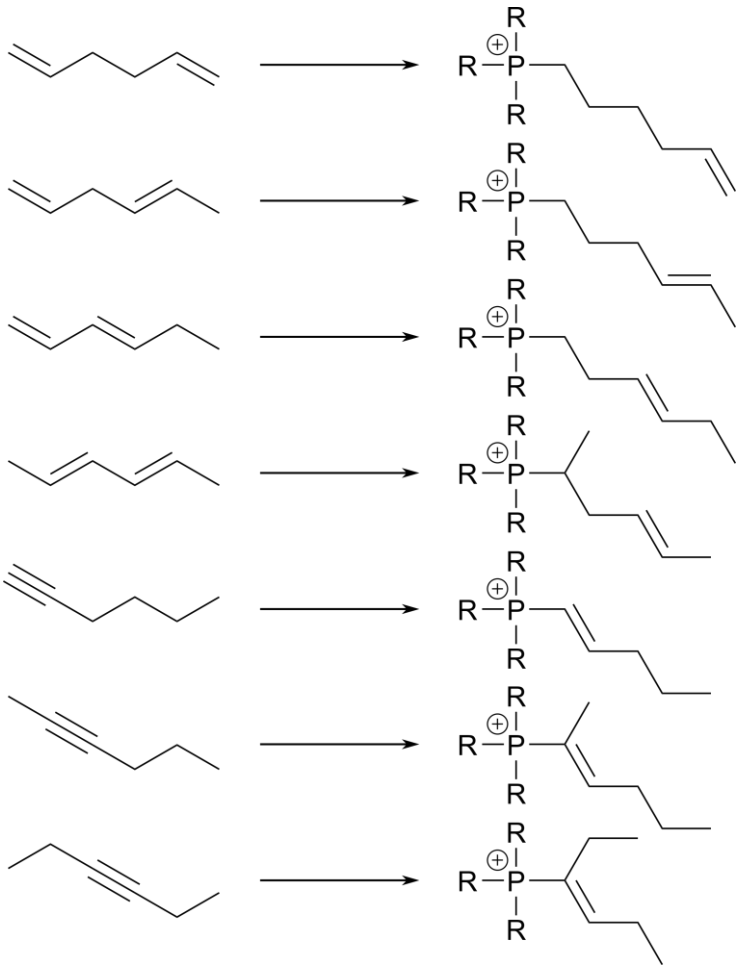

Figure S16. Representative structural isomers formed due to hexadiene and hexyne impurities in 1-hexene. Only the most likely products are depicted. R represents alkyl chains.

Determination of longitudinal relaxation times

T_1 relaxation times were determined using an inversion recovery pulse sequence (T_1ir for bruker software). The intensities were obtained from the integrated peak areas of the assigned signals in the spectrum of untreated C101 (Figure 10). Afterwards, the intensities as a function of relaxation delay time (τ) were fitted using Equation S1.

$$f(\tau) = I_0(1 - ae^{-\tau/T_1}) \quad \text{(S1)}$$

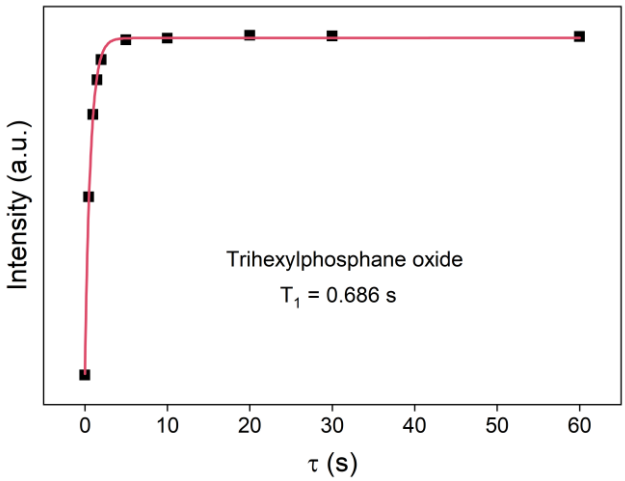

Figure S17. Determination of the T_1 relaxation time for trihexylphosphane oxide.

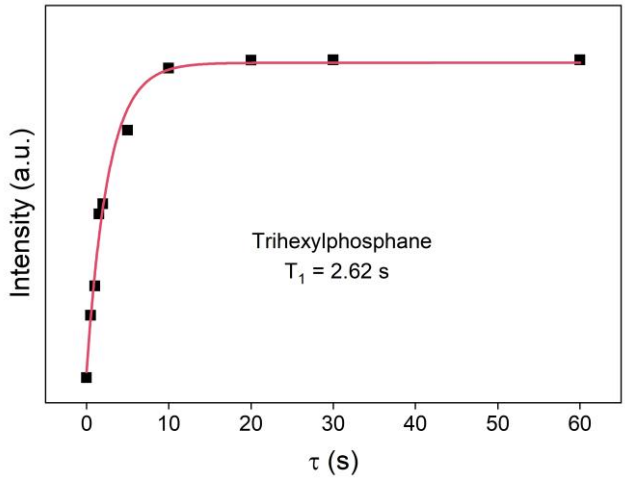

Figure S18. Determination of the T_1 relaxation time for trihexylphosphane.

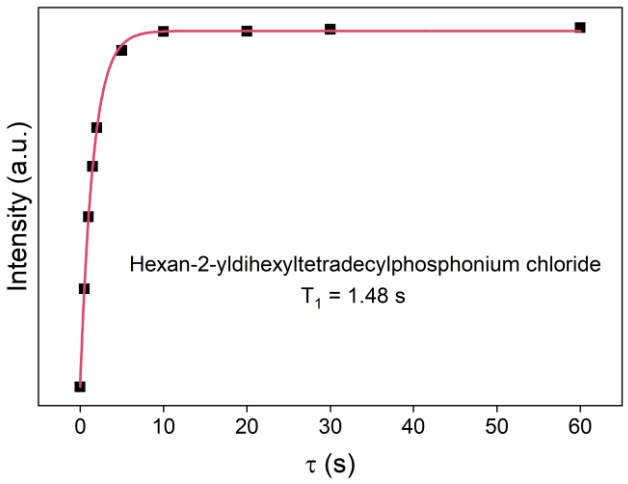

Figure S19. Determination of the T_1 relaxation time for trihexyltetradecylphosphonium chloride.

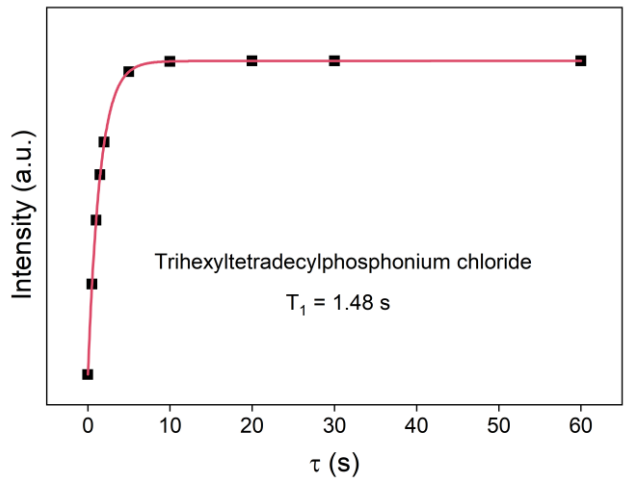

Figure S20. Determination of the T_1 relaxation time for hexan-2-yldihexyltetradecyl phosphonium chloride.

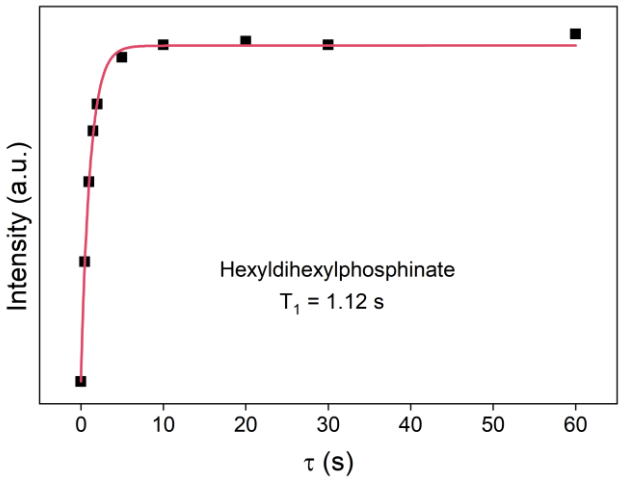

Figure S21. Determination of the T_1 relaxation time for hexyldihexylphosphinate.

^{31}P NMR spectra of $[P_{666}H]^+Cl^-$ and $[P_{666,}H]^+Cl^-$ in C101 at each purification stage

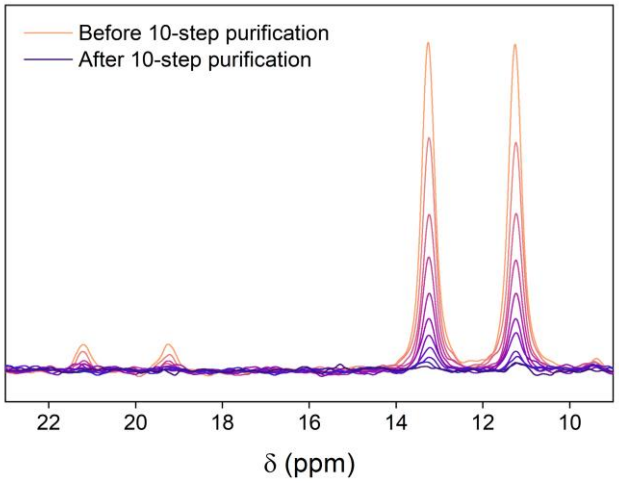

Figure S22. $^{35}P\{^1H\}$ NMR spectra of C101 during a 10-step purification with ethylene glycol solution. Conditions: 200 µL of C101, 250 µL of MeOH, internal reference: 5 wt% H_3PO_4 in D_2O.

Shifting of the trihexylphosphane oxide resonance

Although the overall upfield shift of the trihexylphosphane oxide resonance becomes clear from figure S23, its highly sensitive nature on the exact sample preparation was particularly noteworthy. Hence, the observation of the upfield shift requires careful sample preparation making sure each solution has an identical methanol to C101 ratio. Otherwise, shifts up to 0.5 ppm were observed requiring remeasurements to capture the minor upfield shifting.

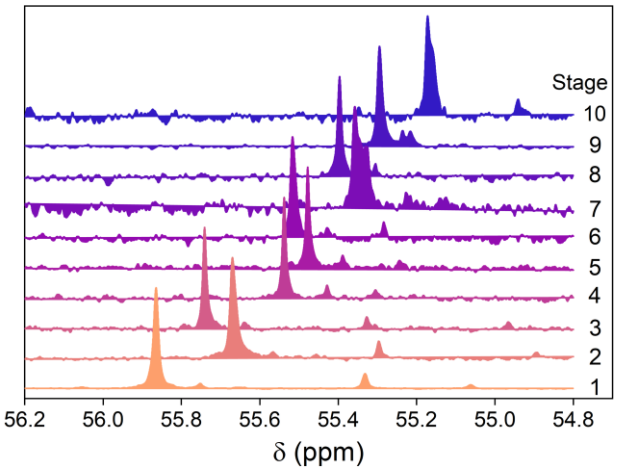

Figure S23. $^{35}P\{^{1}H\}$ NMR spectra of trihexylphosphane oxide in C101 solution at each purification step. Conditions: 200 µL of C101, 250 µL of MeOH; internal reference: 5 wt% H_3PO_4 in D_2O.

MS analysis of dihexylphosphane oxide at each purification step

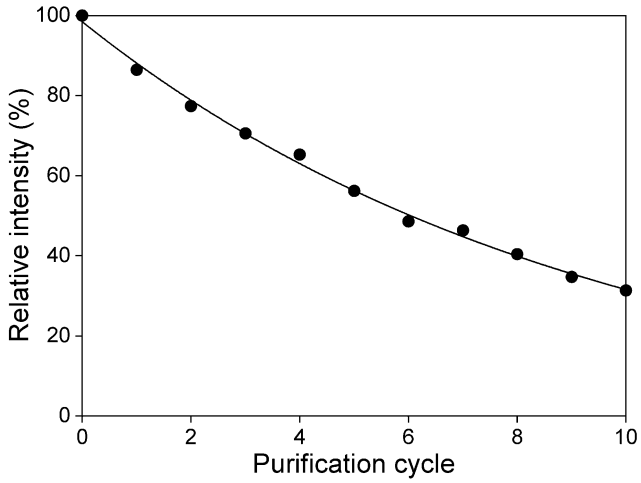

Figure S24. Relative signal intensity of dihexylphosphane oxide during 10 purification cycles based on LC-MS analysis.

Table S2. Composition of C101 after column purification.

Species	Abundancy (%)
Trialkylphosphonium chlorides	0
$P_{66614}Cl$ and isomers	96.9
Hexan-2-yldihexyl tetradecylphosphonium chloride	2.2
Hexyldihexylphosphinate	0
Phosphane oxides	0.9

References

1 J. Meija, T. B. Coplen, M. Berglund, W. A. Brand, P. De Bièvre, M. Gröning, N. E. Holden, J. Irrgeher, R. D. Loss, T. Walczyk and T. Prohaska, *Pure and Applied Chemistry*, 2016, **88**, 293–306.

2 L. McEwana, M. Juliusa, S. Robertsa and J. C. Q. Fletchera, *Gold Bull*, 2010, **43**, 298–306.

3 L. McEwan, University of Cape Town, 2010.